

## SYNTHESIS AND CHARACTERIZATION OF POLYANILINE (PANI) DOPED WITH VANADIUM PENTOXIDE(V<sub>2</sub>O<sub>5</sub>)

S. S. ASHRAF<sup>a\*</sup>, S. ISLAM<sup>b</sup>

<sup>a</sup> *School of Engineering Sciences and Technology, Jamia Hamdard, New Delhi-62, India*

<sup>b</sup> *Department of Physics, Jamia Millia Islamia, New Delhi-25, India*

Conducting polymers are organic macromolecules of electrical properties and lie between metallic and semiconductors. Polyaniline (PANI) / Vanadium pentoxide (V<sub>2</sub>O<sub>5</sub>) composites are conducting polymers which have been synthesized by the technique of polymerization of aniline with vanadium pentoxide (V<sub>2</sub>O<sub>5</sub>) using oxidant ammonium persulphate [(NH<sub>4</sub>)<sub>2</sub>S<sub>2</sub>O<sub>8</sub>]. V<sub>2</sub>O<sub>5</sub> has been added in PANI in three different weight percentages (wt %) i.e. 20, 30 and 40 wt %. Thus the synthesized polymer composites of PANI / V<sub>2</sub>O<sub>5</sub> have been characterized by X-ray diffraction (XRD), Fourier Transform Infrared Spectroscopy (FTIR) and Scanning Electron Microscopy (SEM) techniques. The optical properties have been determined using Ultra Violet Visible (UV-Vis) absorption spectroscopy. DC conductivity of PANI / V<sub>2</sub>O<sub>5</sub> has been carried out. It is found that electrical conductivity ( $\sigma_{dc}$ ) and optical energy band gap ( $E_g$ ) of polymer composites PANI / V<sub>2</sub>O<sub>5</sub> both vary with the varying concentration of V<sub>2</sub>O<sub>5</sub> in PANI. XRD patterns of PANI / V<sub>2</sub>O<sub>5</sub> exhibits the increase in crystallinity with increasing weight percent of V<sub>2</sub>O<sub>5</sub> in PANI which may be attributed to interaction of PANI with V<sub>2</sub>O<sub>5</sub>. SEM images of PANI / V<sub>2</sub>O<sub>5</sub> show the change in surface morphology with varying concentration of V<sub>2</sub>O<sub>5</sub> in PANI.

(Received February 12, 2020; Accepted July 9, 2020)

*Keywords:* PANI/V<sub>2</sub>O<sub>5</sub>, XRD, SEM, UV-Vis and DC conductivity

### 1. Introduction

The conducting polymers are very prominent kind of materials having unique optical, electrical and chemical properties which make them potential candidates for various technological applications. These types of materials when doped, provide wider scope for accessing its electrical property from semiconducting to conducting [1, 2]. Owing to this unique property of these conducting polymers, new models have been developed to study the mechanism of charge transport [3, 4]. These unique properties have led to their emergence as new kind of materials.

Doping of these conducting polymers with oxides enables it to transform from semiconducting to conducting mode which results in transportation of charge. Amongst various kind of conducting polymers, polyanilines are studied widely due to its easier synthesis in aqueous media and are environmentally stable. Polyaniline (PANI) and its derivatives have wide technological applications because of their high electrical conductivity and reversible proton doping. It is also easier to prepare it in bulk. In recent years PANI derivatives have engaged the increasing attention of many researchers due to its wide applications in making humidity sensors [7–10]. Its electrical conductivity is reported to be strongly dependent on the doping level, redox state and moisture content [11]. One of the PANI's derivatives has been Poly(o-toluidine) (POT) which is also a conducting polymer. It has wide applications in batteries, sensors and electronic devices [12].

POT possesses higher processibility and solubility as compared to PANI. The efforts have been made to harmonize the mechanisms of process of aniline oxidation with the corresponding properties of POT like electrical conductivity, crystallinity and molecular weight. However their optical, dielectric and electrical properties get varied when taken in the composite form. Many researchers conducted studies on dielectric and electrical conductivity properties of composites

---

\*Corresponding author: shahabash@gmail.com

conducting polymers [8-10]. Recently heterogeneous conducting polymer composites such as organic–inorganic nanocomposites, have been studied extensively because these materials exhibit properties that could not be obtained by the homogeneous components. These composite polymers are potential candidates to be used in photo and electro catalytic systems and chemical current sources. By doping of these materials, quantum fields can be enhanced in these devices.

In our present research we have attempted to increase the properties of PANI doped with vanadium pentoxide ( $V_2O_5$ ). Amongst inorganic dopant, the vanadium pentoxide ( $V_2O_5$ ) is prominently used because of its many applications in electronic devices [19, 20].  $V_2O_5$  exhibits the photovoltaic and photoconductive actions both. In photovoltaic actions, the light energy is directly converted into electricity whereas in photoconductive actions, the electrical resistance decreases with increasing radiance. Doping of conducting polymers is processed by using Lewis acid. Further  $V_2O_5$  is stable in nature and free of any hazardous effects and can be manipulated easily.  $V_2O_5$  has been reported to be able to significantly improve the current efficiency of Organic Field-effect Transistor (OFET) and Organic Light Emitting Diode (OLED)[21]. It has many applications in electro chromic devices, sensors, catalysts and lithium batteries.

The present work attempts to synthesis of polyaniline (PANI) using oxidation polymerization process in aqueous medium and PANI/ $V_2O_5$  polymer composites at three different weight percentages ( 20, 30 and 40 wt %) of  $V_2O_5$  in PANI. DC conductivity of PANI and PANI/ $V_2O_5$  have been determined. The PANI and PANI/ $V_2O_5$  polymer composites have been characterized by X-ray diffraction (XRD) and UV-Visible (UV-Vis) spectrophotometry. Fourier Transform Infrared Spectroscopy (FTIR) analysis of PANI and PANI/ $V_2O_5$  composites have been carried out to observe the structural changes with increasing weight percentage in polymeric chain. Surface morphology of undoped PANI and PANI/ $V_2O_5$  polymer composites has been carried out using SEM.

## 2. Experimental

Analytical reagent (AR) chemicals have been used. Polyaniline (PANI) and Polyanilinevanadium pentoxide (PANI/ $V_2O_5$ ) composites have been synthesized by polymerization technique using oxidant ammonium persulphate[( $NH_4$ )<sub>2</sub> S<sub>2</sub>O<sub>8</sub>] in aqueous medium. In this process 0.1 mole of aniline was dissolved in 1 mole of HCl acid. Further, 0.1 mole of ammonium persulphate[( $NH_4$ )<sub>2</sub> S<sub>2</sub>O<sub>8</sub>] was added in the obtained solution. It was stirred continuously for 5–6 hrs at 2–6 °C temperature. Once the aniline get dissolved in ( $NH_4$ ) S<sub>2</sub>O<sub>8</sub>) solution, the colour of the solution becomes green. Thus polymerization reaction get started. The mixture of oxide and PANI were taken out and washed out in distilled water. Thus obtained precipitates were put in oven for 22 - 24 hours to get homogeneity. The homogenous precipitates were washed in tetra hydro furan to remove the last traces of unreacted PANI. The oxide in varying weight percentages (20, 30 and 40 wt %) was added in water and added on polyaniline (PANI) solution and stirred continuously so that vanadium pentoxide ( $V_2O_5$ ) can be dropped in the solution. Then (PANI/ $V_2O_5$ ) composites were filtered out. Now these composites were dried in oven for almost 24 hrs. After this these composites were undergone vacuum dried at 65–75°C temperature for 1-2 hrs. The characterization of obtained composites have been carried out using XRD, SEM, FTIR and UV-Vis.

The bulk samples of polymer composites PANI/ $V_2O_5$  were grinded in order to get in powder form and then compressed at a pressure of about 6.5 to nn to make pellets. The dc conductivity of pellets composites have been measured using two-probe technique method at temperature lies between 250–500<sup>0</sup>K. Inside metallic sample holder, between the electrodes made up of steel, the pellets of PANI and PANI/ $V_2O_5$  were mounted then dc voltage 1.5 V applied across electrodes. The corresponding current was determined using Keithley Electrometer Model 6157A and the corresponding temperature with a copper–constantan thermo-couple[21, 22].

X-ray diffraction (XRD) analysis of PANI/ $V_2O_5$  composites polymers was carried out through Panalytical (PW 3710) X-ray diffractometer instrument. The composites were analysed in diffraction angle range of 0–90<sup>0</sup> with scan speed of 0.2<sup>0</sup>/sec. Ultra-violet Visible (UV-Vis) Spectroscopy of composites have been carried out using CamSpec M550 UV-Vis

Spectrophotometer. The FTIR of composites polymers have been carried out by PerkinElmer FTIR spectrometer in frequency range 300 - 5000  $\text{cm}^{-1}$ . SEM was carried out to study the morphology of the polymer composites.

### 3. Results and discussion

#### 3.1. DC conductivity

The dc conductivity derives from the charge carriers flowing into the  $\pi$ -electronic system by process of doping [23]. DC conductivity ( $\sigma_{dc}$ ) of polymer composites PANI/ $\text{V}_2\text{O}_5$  has been carried out at a constant 1.5 V dc voltage and at temperature lying between 250 – 500<sup>0</sup>K. The temperature dependent conductivity is represented by the relation given below [24, 25]

$$\sigma_{dc} = \sigma_0 \exp(-\Delta E_a/kT) \quad (1)$$

or,

$$\ln \sigma_{dc} = -\Delta E_a/kT + \ln \sigma_0 \quad (2)$$

Here  $\Delta E_a$  is called activation energy.  $k$  and  $\sigma_0$  are known as Boltzmann constant and pre-exponential factor and respectively. This is Arrhenius type equation. Temperature dependent electrical conductivity of composite polymers at three different weight percentages (20, 30 and 40 wt %) of  $\text{V}_2\text{O}_5$  are shown in Fig. 1.

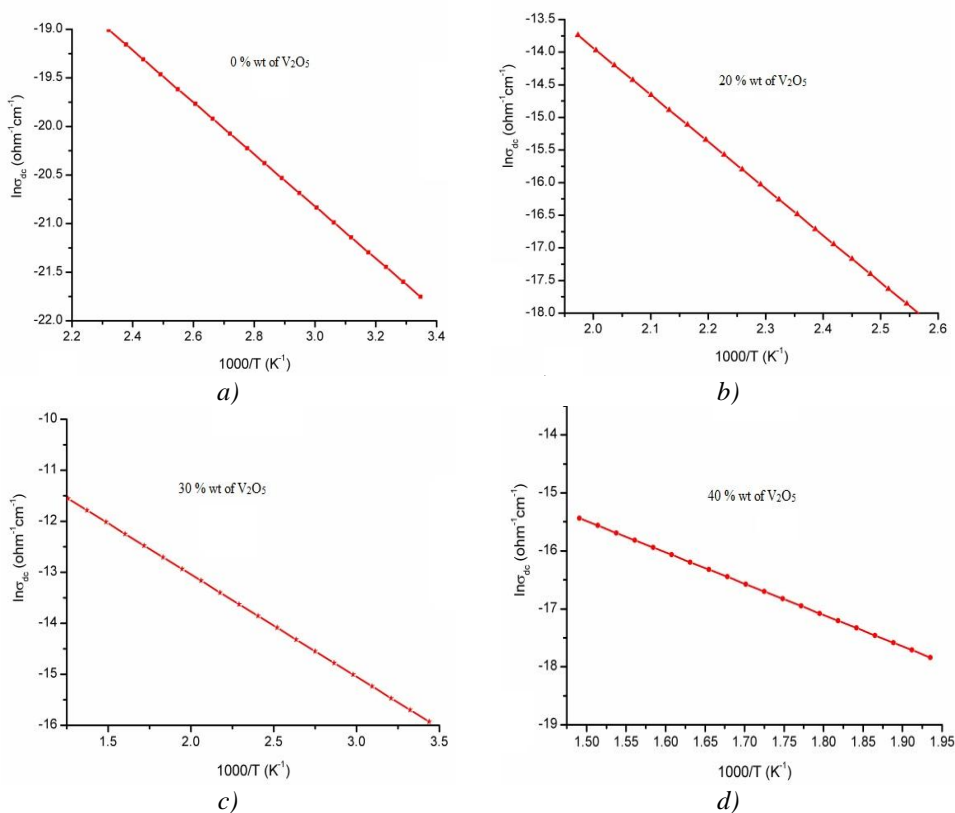


Fig.1 Graph between  $1000/T$  ( $\text{K}^{-1}$ ) versus  $\ln \sigma_{dc}$  ( $\text{ohm}^{-1}\text{cm}^{-1}$ ) of PANI/  $\text{V}_2\text{O}_5$  composites at three different weight percentages (20, 30 and 40 wt %) of  $\text{V}_2\text{O}_5$ .

The plots between  $1000/T$  ( $K^{-1}$ ) versus  $\ln\sigma_{dc}$  ( $ohm^{-1}cm^{-1}$ ) give straight line and slopes of these graphs give activation energy ( $\Delta E_a$ ) are. This exhibits that conduction mechanism have taken place in the doped PANI samples ie PANI/  $V_2O_5$ . Doping with  $V_2O_5$  in PANI inserts charge carriers in electronic structure of PANI/  $V_2O_5$ . The interaction between electron with nuclei results in carrier delocalization in polymeric chain. Therefore, doping with  $V_2O_5$  introduces charge transfer and counter ion. It also controls the Fermi energy. The carrier concentration increases and therefore charge carriers that lead to increase in conductivity of the composite polymers. As the slope of the straight line increases with increasing weight percentage of  $V_2O_5$  upto 30 wt% and then increases at 40 wt %. Therefore, the corresponding conductivity ( $\sigma_{dc}$ ) of the and the activation energy ( $\Delta E_a$ ) of PANI/  $V_2O_5$  increases up to 30 wt % and then starts decreasing at 40 weight % of  $V_2O_5$ . The charge carriers are self-localized at lower doping levels and therefore they form nonlinear configurations. Due to higher value of inter-chain transfer integrals, charge transportation may be along the conjugated chains as a result of inter-chain hopping [25- 27]. The wave functions are delocalized along the polymeric chain over several lattice constants if the polymer composites are heavily doped (40 weight %). Because of degenerate ground states, dominant charge carriers in ployaniline (PANI) are bipolarons and polarons. Once PANI was doped with vanadium pentoxide ( $V_2O_5$ ), the charge carriers formed the nonlinear configurations, thus not bringing any substantial change in the conductivity. The nonlinear formation in PANI/  $V_2O_5$  occurs more in heavy doping (40 wt %  $V_2O_5$ ) which can be considered a reason for it to exhibit lesser conductivity than 20 wt % and 30 wt % doped polymer. The variation of electrical conductivity ( $\sigma_{dc}$ ) and corresponding activation energy ( $\Delta E_a$ ) with increasing concentration of  $V_2O_5$  are shown in Fig. 2.

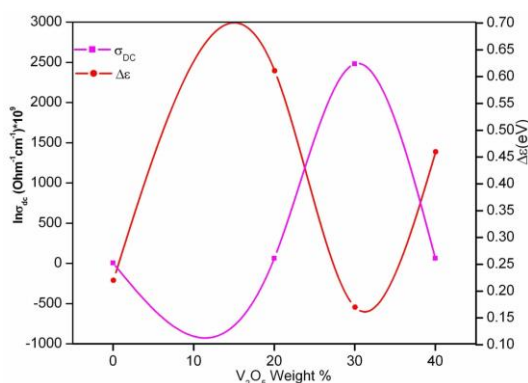


Fig.2. Plot of electrical conductivity  $\ln\sigma_{dc}$  and activation energy ( $\Delta E_a$ ) at different weight % of  $V_2O_5$ .

The above figure exhibits that activation energy ( $\Delta E_a$ ) initially increases with increasing dopant concentration. This may occur due of increment in carrier concentration and the possible change in Fermi energy. The increase in  $\Delta E_a$  may not be necessarily due to conductivity mechanism taking place in extended states far above mobility edge or by the process of hopping in localized states. This can be explained on the basis of Davis and Mott Model which suggests that pre- exponential factor ( $\sigma_0$ ) in extended band must be greater by two or three orders to that of conduction in localized band [24]. In this case the value of  $\sigma_0$  is of the order of  $10^3$ -  $10^4$   $ohm^{-1}cm^{-1}$  which exhibits that conduction occurs due to excitation of charge carriers into extended state. Another reason for this conduction to take place is process of hopping because of presence of wider localized states near Fermi level. Thus the conduction through extended state does not occur. The observed values of activation energy ( $\Delta E_a$ ), pre exponential factor ( $\sigma_0$ ) and dc conductivity ( $\sigma_{dc}$ ) are given in Table 1.

Table 1. Values of dc conductivity ( $\sigma_{dc}$ ) pre exponential factor ( $\sigma_0$ ) and activation energy ( $\Delta E_a$ ) with increasing concentration of  $V_2O_5$  in PANI.

| Sample                    | $\sigma_{dc}(\Omega^{-1} \text{ cm}^{-1})$ | $\sigma_0(\Omega^{-1} \text{ cm}^{-1})$ | $\Delta E_a(\text{eV})$ |
|---------------------------|--|---|-------------------------|
| Undoped PANI              | $3.21 \times 10^{-9}$                      | $2.39 \times 10^{-6}$                   | $23.0 \times 10^{-2}$   |
| PANI/ $V_2O_5$ at 20 wt % | $6.37 \times 10^{-8}$                      | $2.01 \times 10^{-1}$                   | $21.1 \times 10^{-2}$   |
| PANI/ $V_2O_5$ at 30 wt % | $2.13 \times 10^{-6}$                      | $1.12 \times 10^{-4}$                   | $19.2 \times 10^{-2}$   |
| PANI/ $V_2O_5$ at 40 wt % | $8.27 \times 10^{-7}$                      | $4.16 \times 10^{-4}$                   | $43.2 \times 10^{-2}$   |

### 3.2. UV-Visible and dielectric studies

In UV-Vis absorption spectrum, the optical band gap ( $E_g$ ) can be determined by using Tauc's relation [26,27] which is given as:

$$\alpha h\nu = A (h\nu - E_g)^n \quad (3)$$

where A is a constant, called band tailing parameter and  $E_g$  is called optical band gap. The index 'n' is associated with the type of transition which has values 1/2 and 2 for direct and indirect transitions respectively. In present study, the transition taking place is indirect.

The absorption coefficient ( $\alpha$ ) can be determined using the relation given below:

$$\alpha = \text{optical density (O.D.)} / \text{thickness of the film} \quad (4)$$

and the value of extinction coefficient (k) can be written as

$$k = \alpha \lambda / 4\pi, \quad (5)$$

where  $\lambda$  is incident photon's wavelength.

The optical band gap ( $E_g$ ) of undoped (PANI) and doped (PANI/ $V_2O_5$ ) can be measured from the graph between  $(\alpha h\nu)^{1/2}$  versus incident energy ( $h\nu$ ) shown in Fig. 3 [28,29].

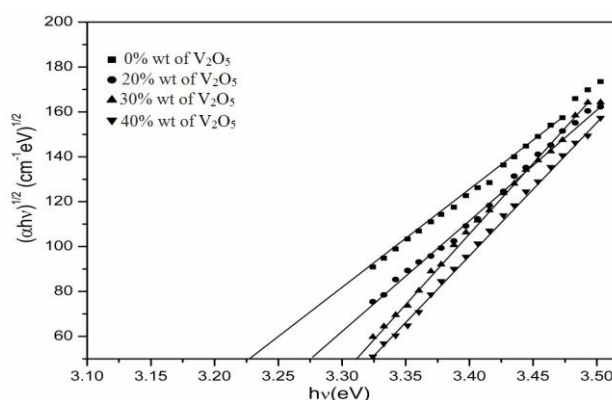


Fig.3. Graph of  $(\alpha h\nu)^{1/2}$  versus incident energy ( $h\nu$ ) at varying weight % of  $V_2O_5$ .

The slopes of graph give the optical energy (band gap  $E_g$ ). From the above observations it is found that  $E$  increases with increasing weight percentage of  $V_2O_5$ . The observed values of  $E_g$  and  $k$  at different  $V_2O_5$  weight percent are given in Table 2. The absorption spectrum depends on the atomic short range order and defects associated with them. The optical energy of composite polymers increases with incorporation of  $V_2O_5$  in PANI which may occur due to increase of disorderness in the system and consequently density of defect states decreases. Therefore, it may be concluded that polyaniline doped with  $V_2O_5$  has tremendous impact on the optical parameters of PANI. Since indirect transition takes place, therefore the values of activation energy (electronic band gap) and optical energy differ in optical study. This type of transition is a two-step process in which an electron absorbs photon ( $h\nu$ ) and phonon as well. The photon supplies the minimum energy required to make transition and the phonon imparts momentum. Since the electronic band gap (activation energy) is the minimum energy required to excite the electrons from valence band to conduction band therefore the electronic band gap has values less than the optical energy (band gap) [27]. The UV-Vis absorption spectrum in wavelength 500-1100 nm is given in Fig. 4.

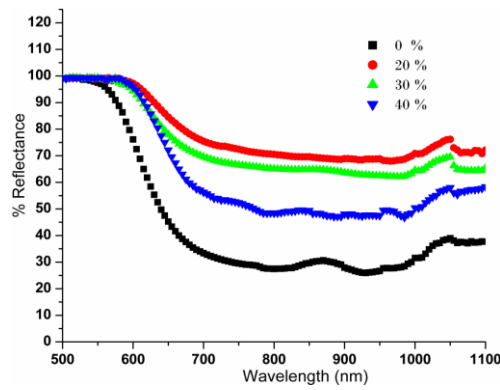


Fig. 4. Graph between wavelength and reflectance at different weight % of  $V_2O_5$ .

From the above UV-Vis absorption spectrum, the dielectric constant ( $\epsilon'$ ), dielectric loss ( $\epsilon''$ ) and refractive index ( $n$ ) have been measured. The values of refractive index ( $n$ ) have been determined by using the theory of reflectivity of light. According to this theory, the reflectance of light can be written in terms of Fresnel's coefficient. Further the reflectivity in terms of refractive index can be expressed as

$$R = [(n-1)^2 + k^2] / [(n+1)^2 + k^2] \quad (6)$$

and  $\alpha = 4\pi k/\lambda$ , where  $\lambda$  is wavelength of the incident photon

The values of dielectric constant ( $\epsilon'$ ) and dielectric loss ( $\epsilon''$ ) can be measured using relation given below [26]

$$\epsilon' = n^2 - k^2 \quad (7)$$

and

$$\epsilon'' = 2nk \quad (8)$$

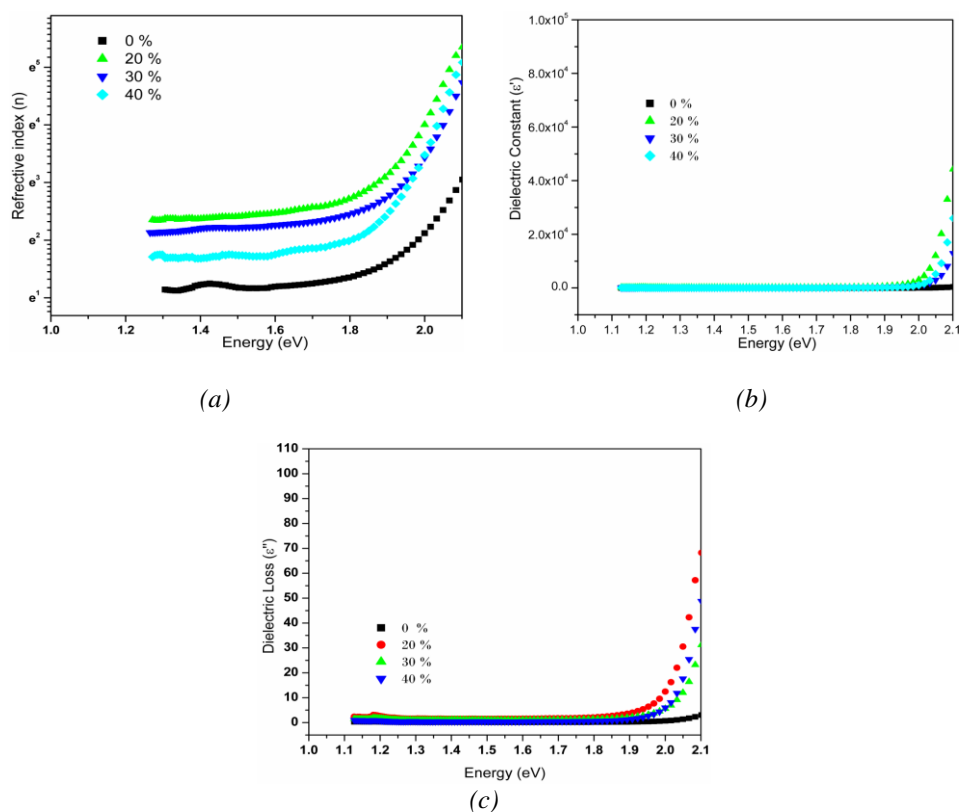


Fig. 5. (a). Graph between Refractive index versus photon energy ( $h\nu$ ) at different weight % of  $V_2O_5$ ; (b). Graph between dielectric constant ( $\epsilon'$ ) versus photon energy ( $h\nu$ ) at different weight % of  $V_2O_5$ ; (c) Graph between dielectric loss ( $\epsilon''$ ) versus photon energy ( $h\nu$ ) at different weight % of  $V_2O_5$

The refractive index ( $n$ ), dielectric constant ( $\epsilon'$ ) and dielectric loss ( $\epsilon''$ ) versus photon energy ( $h\nu$ ) have been plotted and it is shown in Fig. 5a, b and c.

Table 2. Values of optical band gap ( $E_g$ ), real and imaginary parts of dielectric constants ( $\epsilon'$ ,  $\epsilon''$ ) and refractive index ( $n$ ) at varying weight % of  $V_2O_5$  at temperature  $450^\circ K$  and wavelength  $620\text{ nm}$ .

| Sample                         | $E_g$ (eV) | $\epsilon'$        | $\epsilon''$ | $n$   |
|--------------------------------|------------|--------------------|--------------|-------|
| PANI/ $V_2O_5$ at 0% $V_2O_5$  | 3.19       | $2.28 \times 10^4$ | 7.57         | 8.34  |
| PANI/ $V_2O_5$ at 20% $V_2O_5$ | 3.41       | $1.40 \times 10^5$ | 56.45        | 54.78 |
| PANI/ $V_2O_5$ at 30% $V_2O_5$ | 3.27       | $1.40 \times 10^5$ | 56.54        | 30.99 |
| PANI/ $V_2O_5$ at 40% $V_2O_5$ | 3.29       | $1.39 \times 10^5$ | 56.34        | 32.39 |

It is evident from the Figs. 5(a), 5(b) & 5 (c) that refractive index ( $n$ ) and dielectric constant ( $\epsilon'$ ) of PANI/ $V_2O_5$  composites both exponentially increase with the increasing incident energy ( $h\nu$ ). The higher values of dielectric constant ( $\epsilon'$ ) and dielectric loss ( $\epsilon''$ ) are accounted for large content of oxide present in  $V_2O_5$ . Because of this the crystallinity increases with increasing oxide. This can be seen in XRD pattern of PANI/ $V_2O_5$  shown in Figure 7. This results in increasing interfacial interactions between polyaniline and vanadium pentoxide that may lead to

maximum polarization of space charge Because of static dielectric permittivity, the dielectric constant is produced which may be written as

$$\epsilon_s = C_{gb}/C_0 \quad (9)$$

where,  $C_{gb}$  is called grain boundary capacitance. Dielectric constant depends on  $C_{gb}$ . The values of grain conductivity increases with the increasing concentration of vanadium pentaoxide in polyaniline. The increase in charge carrier concentration results in increase grain boundary capacitance ( $C_{gb}$ ). The size of the grains also increases with increasing concentration of  $V_2O_5$ . Therefore the increment of grain size and grain boundary capacitance results in increase in dielectric constant. When concentration of  $V_2O_5$  in PANI is below 40% then they exhibits decrease in dielectric constant and conductivity both due to poor interface between the polymers. Also they exhibits no change in value of dielectric constant in visible region. The change is only exhibited in Ultra-Violet region[30].

### 3.3. FTIR analysis

In FTIR spectrum, change in the functional groups are observed. There are two types of regions in this spectrum, one is called finger print region (0 to  $1000\text{ cm}^{-1}$ ) and another one is called functional group region ( $1000\text{ cm}^{-1}$  to  $4500\text{ cm}^{-1}$ ). Fig. 6 shows FTIR spectrum of PANI/ $V_2O_5$  at different weight % of  $V_2O_5$  in PANI.

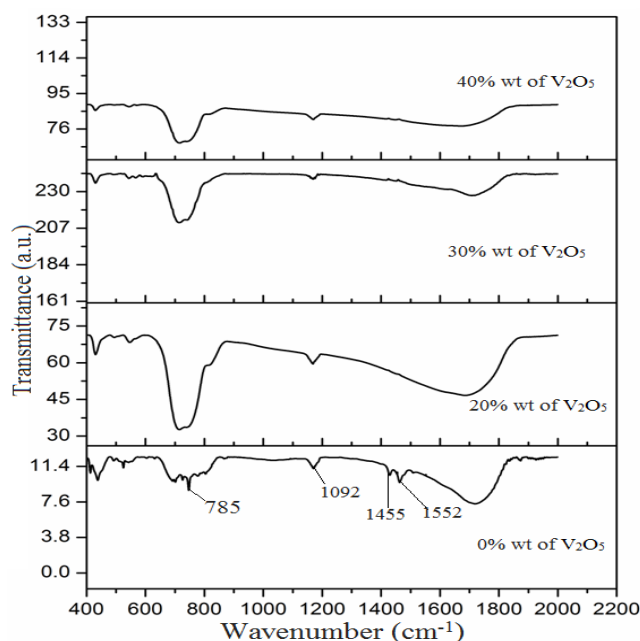


Fig. 6. FTIR patterns of PANI/  $V_2O_5$  at different weight % of  $V_2O_5$ .

From the above bands we can observe characteristics peaks of nitrogen quinoid ring (Q) in the range of  $1572\text{--}1592\text{ cm}^{-1}$  with decreasing broadening at increasing concentration of  $V_2O_5$  [31]. On the basis of vibration theory of PANI and its derivatives we can say that the position of this band indicates the degree of oxidation in polymer PANI/  $V_2O_5$ . This band appears because of superposition of vibrations of C-C stretching in benzene ring (B). The observed characteristic peaks around  $1455\text{ cm}^{-1}$  and  $1552\text{ cm}^{-1}$  can be attributed to the stretching in the vibrations of N B N and N Q N rings respectively. The band observed at  $1486\text{ cm}^{-1}$  is due to C-H stretching of secondary aromatic amine and the band found at  $1091\text{ cm}^{-1}$  may be attributed to the characteristic peak of bond B-NH-B or B-NH-Q bending in the plane modes.

The substituted benzene rings corresponding to deformations of C-H are allocated to band at  $785\text{ cm}^{-1}$ . These are in good agreement with Bormashenko et al [31]. With the increasing

weight % of  $V_2O_5$  in PANI, the alkynes are formed corresponding to the  $1678\text{--}1686\text{ cm}^{-1}$  which results in  $C = C$  stretch. The re-orientation of molecular bonds are required to make alkyne formation. It requires huge amount of energy which is supplied during breaking of  $C - H$  and  $C - C$  bonds. To trigger alkyne formation, excitation energy should be greater than the threshold energy. Since in our study we get greater value of excitation energy than the threshold therefore, alkyne formation takes place and consequently  $\pi$  electrons are delocalized which results in making of triple bonds.

The comparison between doped PANI/  $V_2O_5$  and undoped PANI spectrum exhibits shift in Quinoid peaks from  $1089\text{ cm}^{-1}$  to  $1071\text{ cm}^{-1}$  and  $1482\text{ cm}^{-1}$  to  $1474\text{ cm}^{-1}$ . This shift in peaks of doped PANI/  $V_2O_5$  in FTIR study indicates the formation of more ions during doping. The alkyne formation started taking place beyond doping of 20 % and above [32]. This shows that the triple bonds formations affect the semi-conducting properties of the doped PANI/  $V_2O_5$  polymer. Hence the semi-conducting nature of the doped PANI/  $V_2O_5$  polymers increases despite alkyne formation.

### 3.4. XRD analysis

XRD patterns of undoped PANI exhibits the amorphous nature as there is no sharp peak observed [34, 35] whereas the XRD patterns of  $V_2O_5$  doped PANI confirms the semi-crystalline nature of doped samples as shown in Fig.7.

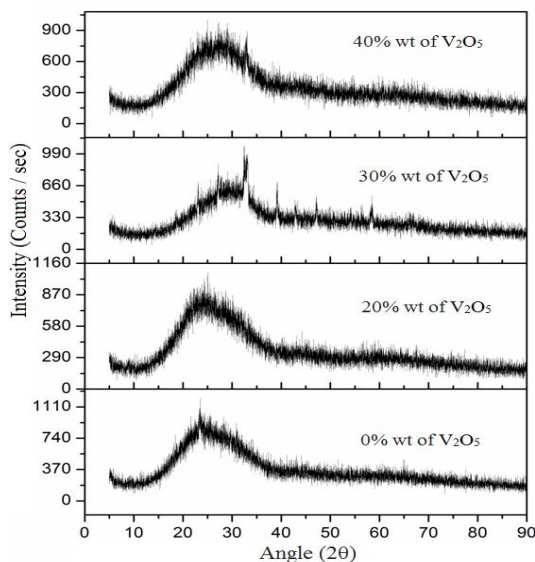


Fig. 7. The XRD patterns of PANI/  $V_2O_5$  at different weight % of  $V_2O_5$ .

In undoped PANI (0% of  $V_2O_5$ ) sample, the amorphous hump is found at  $23^{\circ}$ – $26^{\circ}$  which gets shifted towards lower angle at  $13\text{--}17^{\circ}$  in  $V_2O_5$  doped PANI samples. In 20 weight % of  $V_2O_5$  doped samples, three other small peaks appears near  $15^{\circ}$  (200),  $20^{\circ}$  (001) and at  $26^{\circ}$  (110), which confirm the presence of  $V_2O_5$  in PANI. These three peaks are continuously appearing up to 40 weight % of  $V_2O_5$  in PANI. Thus it is found that  $V_2O_5$  dopant interacts well with PANI which results in continuously increasing conductivity and crystallinity of the composites PANI/  $V_2O_5$ . This increasing crystallinity of the composites PANI/  $V_2O_5$  may be attributed to polymer chain alignment or because of making of single or multiple helices [36, 37].

### 3.5. SEM analysis

The Scattering Electron Microscope (SEM) study of PANI/  $V_2O_5$  helps us to analyse the effect on morphology of PANI when it is doping with  $V_2O_5$ . In the current analysis it is found that increase in weight percentage of dopant  $V_2O_5$  in PANI exhibits the change in surface morphology of composite polymers PANI/  $V_2O_5$  shown in Fig.8 [38].

Further  $V_2O_5$  appears to be dispersed in composite polymer PANI/ $V_2O_5$  as shown in Fig. 8 (b). With the higher concentration of dopant  $V_2O_5$  in PANI, the clusters are formed as shown in Fig. 8(c) which results in higher value of conductivity. With the increasing weight % of  $V_2O_5$  in PANI upto 40%, the particle size appears to get reduced as shown in Fig. 8 (d) which may be attributed to breaking up of clusters. Therefore it is concluded that higher concentration of  $V_2O_5$  in PANI does not necessarily increase the size of the particles.

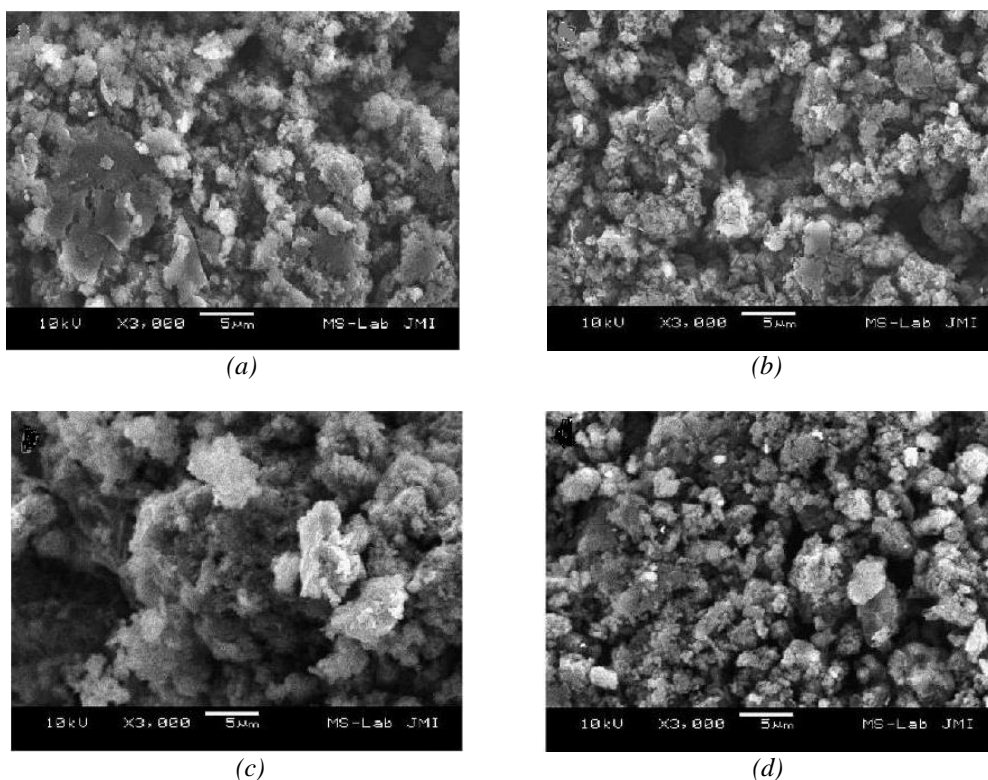


Fig. 8. SEM Images of PANI/  $V_2O_5$  composite polymers at different weight % of  $V_2O_5$ .

#### 4. Conclusions

In our study, polyaniline vanadium pentaoxide (PANI/  $V_2O_5$ ) composites at different weight percentage of  $V_2O_5$  have been synthesized by oxidative polymerization technique using oxidant ammonium persulphate  $[(NH_4)_2 S_2O_8]$  in aqueous medium. It is observed that doping with  $V_2O_5$  in PANI causes change in the structural, optical and electrical properties of PANI. From dc conductivity analysis it is found that conductivity of PANI/  $V_2O_5$  polymer composites increases with increasing dopant  $V_2O_5$  concentration in PANI up to three orders of magnitude which indicates the semi-conducting nature of PANI/  $V_2O_5$ . It may be suggested that conduction takes place because of present of large range of localized state in polymer composites PANI/  $V_2O_5$ . XRD analysis of PANI/  $V_2O_5$  at different weight percentage shows the increase in crystallinity with increasing concentration of  $V_2O_5$ .

FTIR spectra confirm the presence of  $V_2O_5$  in polymer chain and exhibits the structural changes in PANI with  $V_2O_5$  doping. UV-Visible analysis shows the presence of indirect bandgap within the polymer composites which increases with increasing weight % of  $V_2O_5$ . These PANI/  $V_2O_5$  polymer composites show the large values of real and imaginary parts of dielectric constant and dielectric loss with doping. SEM analysis polymer composites exhibits the change in surface morphology of PANI doped with  $V_2O_5$  at different weight percent.

## References

- [1] Alan G. MacDiarmid, Arthur J. Epstein, *Synthetic Metals* **69**(1-3), 85 (1995).
- [2] A. B. Kaiser, C. K. Subramaniam, P. W. Gilberd, B. Wessling. *Synthetic metals* **69**(1-3), 197 (1995).
- [3] Teboho Clement Mokhena, Mokgaotsa Jonas Mochane, Jeremia Shale Sefadi, Setumo Victor Motloug, Dickson MuberaAndala, *Impact of Thermal Conductivity on Energy Technologies*, 181 (2018).
- [4] M. Angelopoulos, A. Ray, A. G. MacDiarmid, A. J. Epstein, *Synthetic Metals* **21**, 12 (1987).
- [5] N. Kumar, S. R. Vadera, Jeevan Singh, G. Das, S. C. Negi, P. Aparna, A. Tuli, *Defence Science Journal* **46**(2), 91 (1996).
- [6] S. Wang, L. Sun, Z. Tan, F. Xu, Y. Li, *Journal of thermal analysis and calorimetry* **89**(2), 609 (2006).
- [7] Younan Xia, Joanna M. Wiesinger, Alan G. MacDiarmid, Arthur J. Epstein, *Chemistry of Materials* **7**(3), 443 (1995).
- [8] Xingwei Li, Wei Chen, Chaoqing Bian, Jinbo He, Ning Xu, GiXue, *Applied Surface Science* **217**(1-4), 16 (2003).
- [9] Mukul Biswas, Suprakas Sinha Ray, Yunping Liu, *Synthetic metals* **105**(2), 99 (1999).
- [10] Shama Islam, G. B. V. S. Lakshmi, Azher M. Siddiqui, M. Husain, M. Zulfeqar, *International Journal of Polymer Science* 2013 (2013).
- [11] H. H. Zhou, X. H. Ning, S. L. Li, J. H. Chen, Y. F. Kuang, *Thin Solid Films* **510**(1-2), 164 (2006).
- [12] R. L. N. Chandrakanthi, M. A. Careem, *Thin Solid Films* **417**(1-2), 51 (2002).
- [13] Zhanghua Zhou, Naicai Cai, Yunhong Zhou, *Materials Chemistry and Physics* **94**(2-3), 371 (2005).
- [14] X. B. Cao, Yi Xie, S. Y. Zhang, F. Q. Li, *Advanced Materials* **16**(7), 649 (2004).
- [15] G. B. V. S. Lakshmi, Masood Alam, Azher M. Siddiqui, M. Zulfeqar, M. Husain, *Current Applied Physics* **11**(2), 217 (2011).
- [16] Yen Wei, Guang-Way Jang, Kesyin F. Hsueh, Elliot M. Scherr, Alan G. MacDiarmid, Arthur J. Epstein, *Polymer* **33**(2), 314 (1992).
- [17] Vivian Wing-Wah Yam, *Chemical Communications* **9**, 1006 (2006).
- [18] Zishan H. Khan, M. Manzar Malik, M. Zulfeqar, M. Husain, *Journal of physics condensed matter* **7**, 8979 (1995).
- [19] I. Shama, A. M. Siddiqui, M. Husain, M. Zulfeqar, *Int. J. Adv. Res. Sci. Technol* **2**(3), 150 (2013).
- [20] P. M. Grant, I. P. Batra, *Solid state communications* **29**(3), 225 (1979).
- [21] J. Fink, G. Leising, *Physical Review* **B34**(8), 5320 (1986).
- [22] Shuichi Okano, Masakuni Suzuki, Ken Imura, Noboru Fukada, Akio Hiraki, *Journal of Non-Crystalline Solids* **59**, 969 (1983).
- [23] M. Zulfeqar, Shama Islam, G. B. V. S. Lakshmi, M. Husain Azher M. Siddiqui, In *Physics of Semiconductor Devices*, p. 907, Springer, Cham, 2014.
- [24] N. F. Mott, E. A. Davis, *Electronic processes in non-crystalline materials*, 2nd edn. Clarendon, 32 (1979).
- [25] Ashraf, S. S., and M. Zulfeqar. "EFFECT OF BI ADDITIVE ON OPTICAL AND ELECTRICAL PROPERTIES OF QUATERNARY CHALCOGENIDE  $\text{In}_3\text{Te}_7\text{Bi}_x\text{Se}_{90-x}$  THIN FILMS." *Journal of Ovonic Research* Vol 15, no. 6 (2019): 393-400.
- [26] E. A. Davis, N. F. F Mott, *Philosophical Magazine* **22**(179), 0903 (1970).
- [27] G. E. Asturias, A. G. MacDiarmid, R. P. McCall, A. J. Epstein, *Synthetic Metals* **29**(1), 157 (1989).
- [28] Haresh S. Patel, J. R. Rathod, K. D. Patel, V. M. Pathak, R. Srivastava, In *Advanced Materials Research* **665**, 239 (2013).
- [29] S. E. Chapman, N. C. Billingham, S. P. Armes, *Synthetic metals* **55**(2-3), 995 (1993).
- [30] Jayashree Anand, Srinivasan Palaniappan, D. N. Sathyanarayana, *Synthetic metals* **66**(2), 129 (1994).

- [31] N. V. Bhat, D. S. Wavhal, *Journal of applied polymer science* **70**(1), 203 (1998).
- [32] Edward Bormashenko, Roman Pogreb, Semion Sutovski, Alexander Shulzinger, Avigdor Sheshnev, Alexander Gladkikh, *Synthetic metals* **139**(2), 321 (2003).
- [33] Tanu Sharma, Sanjeev Aggarwal, Shyam Kumar, ViK Mittal, P. C. Kalsi, V. K. Manchanda, *Journal of materials science* **42**(4), 1127 (2007).
- [34] Ashraf, S. S., M. Zulfequar, and M. Uddin. "NON-ISOTHERMAL CRYSTALLIZATION KINETICS OF  $\text{In}_4\text{Se}_{96-x}\text{S}_x$  CHALCOGENIDE GLASSES USING DIFFERENTIAL SCANNING CALORIMETRY." *Chalcogenide Letters* 15, no. 4 (2018): 227-235.
- [35] Ashraf, Syed S., M. Zulfequar, and Moin Uddin. "Thermal Analysis of Se-based Chalcogenide Glass." *Recent Innovations in Chemical Engineering (Formerly Recent Patents on Chemical Engineering)* 11, no. 3 (2018): 172-178.
- [36] S. R. Elliott, *Journal of Non-Crystalline Solids* **81**(1-2), 71 (1986).
- [37] Mousa M. A. Imran, N. S. Saxena, D. Bhandari, M. Husain, *Physica Status Solidi A* **181**(2), 357 (2000).
- [38] ASHRAF, SS, and M. ZULFEQUAR. "BISMUTH ADDITIVE NON-ISOTHERMAL CRYSTALLIZATION KINETICS OF  $\text{In}_3\text{Te}_7\text{Bi}_x\text{Se}_{90-x}$ ." *Chalcogenide Letters* 16, no. 12 (2019): 603-614.